Universal expression and dual function of the atypical chemokine receptor D6 on innate-like B cells in mice.

Chris A. H. Hansell, Chris Schiering, Ross Kinstrie, Laura Ford, Yvonne Bordon, Iain B. McInnes, Carl S. Goodyear, and Robert J. B. Nibbs.

Supplementary Figures & Table.

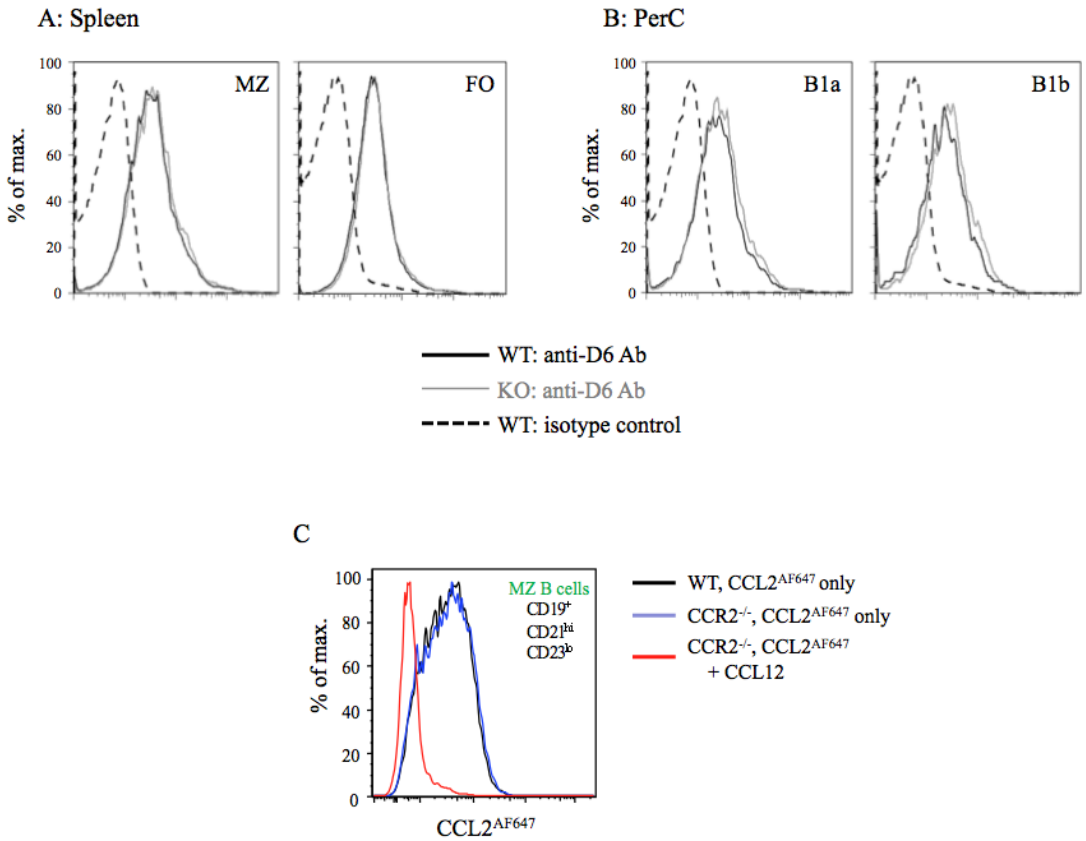

Supplementary Figure 1: D6 detection on IBCs. (A-B) Polyclonal anti-D6 Ab fails to specifically identify WT IBCs. Splenocytes (A) or PerC lavage cells (B) from WT or D6-deficient mice (KO) were incubated at 4°C with polyclonal goat anti-mouse D6 Ab or isotype control Ab, and then at 4°C with fluorescently-labeled anti-goat Ig plus either anti-CD19, -CD21, and -CD23 (spleen) or anti-CD19, -CD11b, and -CD5 (PerC). Cells were analyzed by flow cytometry, with dead cell exclusion. The overlaid histogram plots show anti-D6 and isotype control Ab binding to (A) splenic MZ ($CD19^{+}CD21^{hi}CD23^{lo}$) and FO ($CD19^{+}CD21^{int}CD23^{+}$) B cells, and (B) PerC B1a ($CD19^{+}CD11b^{+}CD5^{+}$) and B1b ($CD19^{+}CD11b^{+}CD5^{-}$) cells. Similar results were seen across a range of anti-D6/isotype Ab concentrations. (C) CCR2 is not required for $CCL2^{AF647}$ uptake by MZ B cells. Single cell splenocyte suspensions from WT or $CCR2^{-/-}$ mice were incubated with 25nM $CCL2^{AF647}$ for 1h at 37°C (+/-250nM CCL12, a D6 and CCR2 ligand), and then with fluorescently-labeled Abs (anti-CD19, anti-CD21, anti-CD23) at 4°C. Cells were analyzed by flow cytometry, with dead cell exclusion, and gated for MZ B cells. Representative, overlaid, $CCL2^{AF647}$ uptake histogram plots are shown. Data are representative of results obtained from at least three independent experiments.

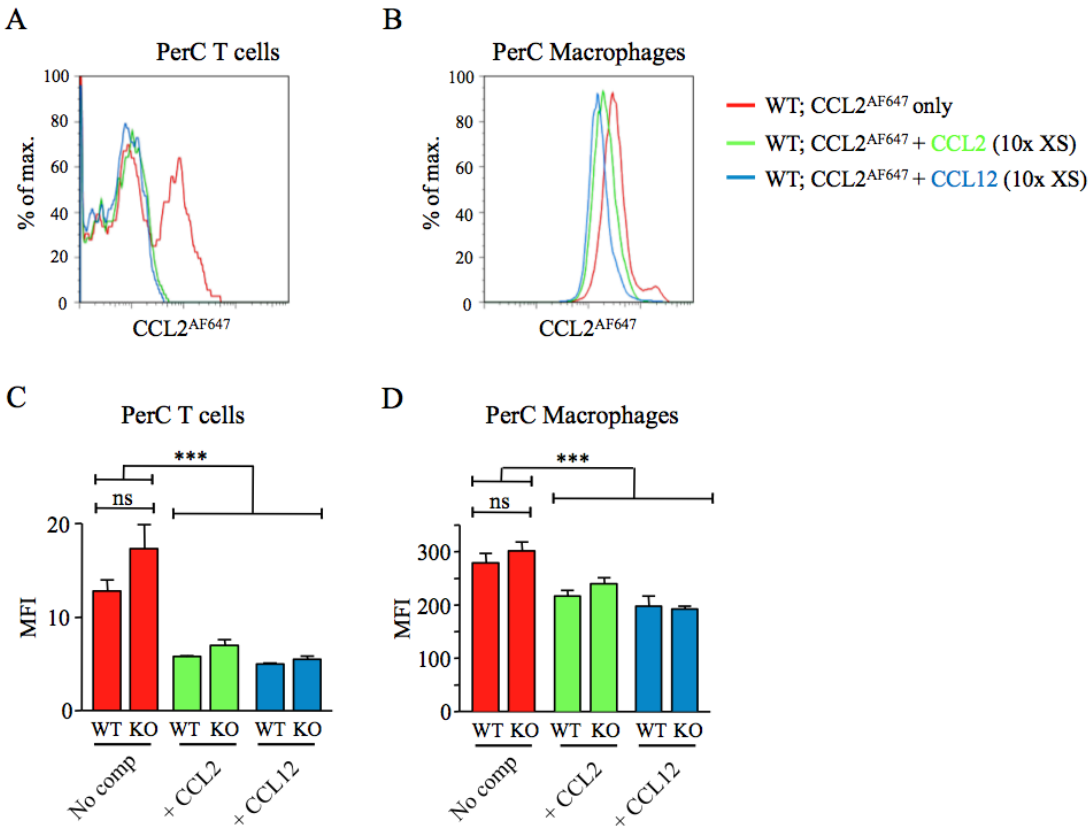

Supplementary Figure 2: $CCL2^{AF647}$ uptake by PerC T cells and macrophages is D6-independent. WT or D6-deficient (KO) PerC cells were incubated at 37°C with 25nM $CCL2^{AF647}$ (+/-250nM CCL2 or CCL12 as indicated), then at 4°C with anti-CD19, -CD11b and -CD5 Abs, and analysed by flow cytometry with dead cell exclusion. T cells were defined as $CD19^{-}CD11b^{-}CD5^{hi}$, and macrophages as $CD19^{-}CD11b^{+}CD5^{-}$. (A-B) Representative, overlaid histogram plots from WT mice. (C-D) Mean+/-SEM mean fluorescence intensity (MFI) values for $CCL2^{AF647}$ uptake by WT and KO cells (4 mice per strain). 'No comp': no unlabelled competitor chemokines. Data shown are representative of results from at least three repeat experiments.

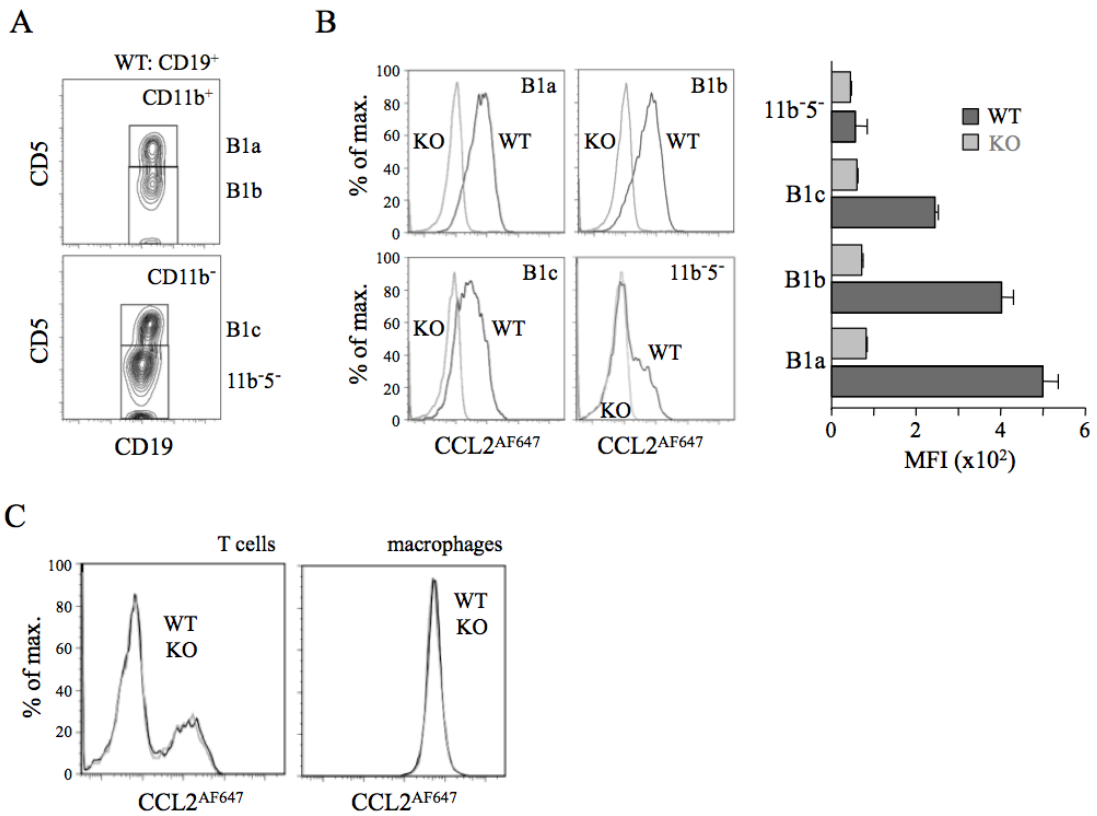

Supplementary Figure 3: PleC B1 cells show D6-dependent CCL2^{AF647} uptake. D6-deficient (KO) or WT PleC cells incubated at 37°C with 25nM CCL2^{AF647}, then at 4°C with anti-CD19, -CD11b and -CD5 Abs, were analysed by flow cytometry with dead cell exclusion. (A) Flow cytometric fractionation of CD19$^+$ PleC cells using Abs against CD11b and CD5. CD19$^+$CD11b$^-$CD5$^-$ cells are labelled '11b$^-$5$^-$'. (B) Overlaid CCL2^{AF647} uptake profiles of WT and KO PerC CD19$^+$ cell subsets identified in A. Bar graph shows the average Mean Flourescence Intensity (MFI) (+/-SEM) of CCL2^{AF647} uptake by these subsets (5 mice per genotype). (C) Overlaid CCL2^{AF647} uptake profiles of WT and KO PleC T cells (CD19$^-$CD11b$^-$CD5^{hi}) and macrophages (CD19$^-$CD11b$^+$CD5$^-$). Results are representative of data from at least three mice per genotype per experiment, with experiments repeated on at least three occasions.

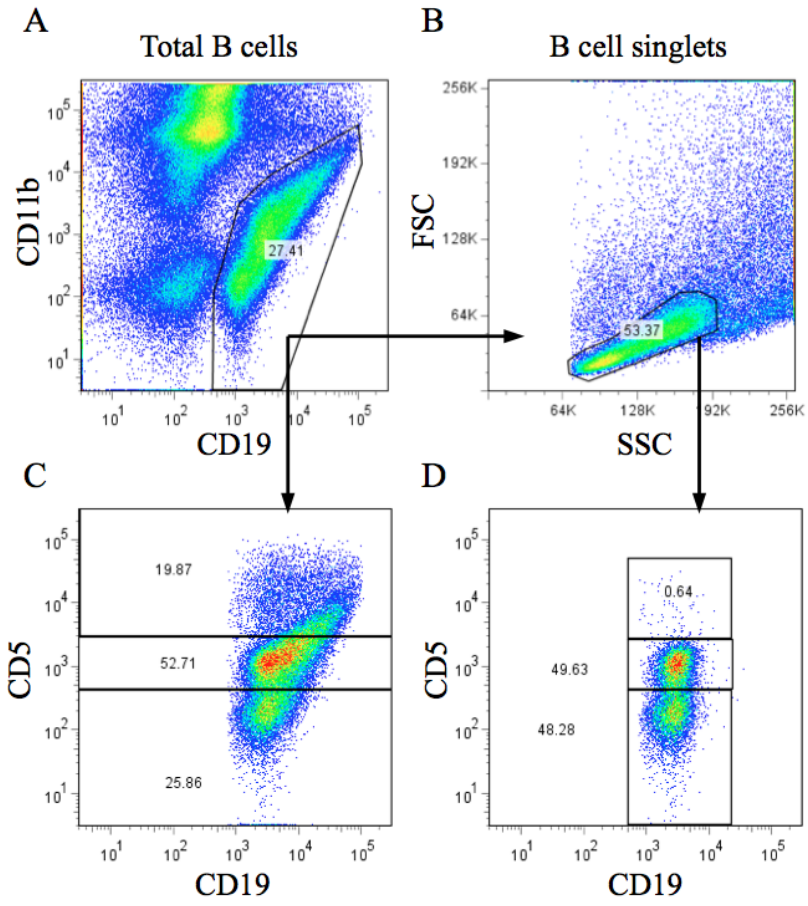

Supplementary Figure 4: Gating strategy excludes dead cells and lymphocyte doublets/aggregates. Dead cells are excluded according to low FSC characteristics and high DAPI staining. (A) B cells are identified as $CD19^{+}CD11b^{+/-}$. (B) B cell 'singlets' are enriched by gating for low FSC and low/moderate SSC. (C-D) Gating strategy removes the $CD19^{+}CD5^{hi}$ population, which, based on co-expression of T cell markers (data not shown), predominantly consists of T cell/B cell conjugates.

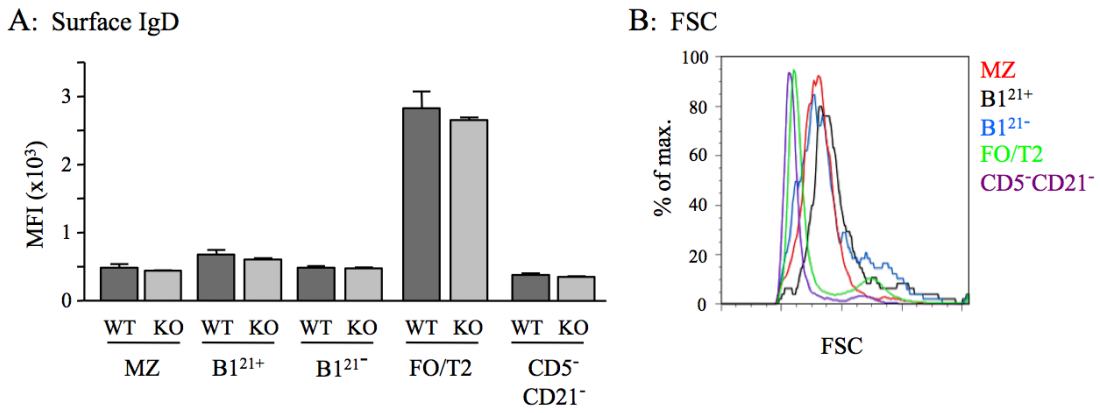

Supplementary Figure 5: Splenic B1 and MZ B cells are larger than other splenic B cells, and express low surface IgD. (A) Mean fluorescence intensity (MFI) of anti-IgD staining of WT and D6-deficient (KO) splenic B cell subsets (identified as in Figure 5C). Data are expressed as mean+/-SEM; 4 mice per genotype. (B) Representative FSC profiles of B cell subsets from WT spleen. 'CD5$^-$CD21$^-$' refers to IgM^{hi}CD23^{lo}CD5$^-$CD21$^-$ B cells.

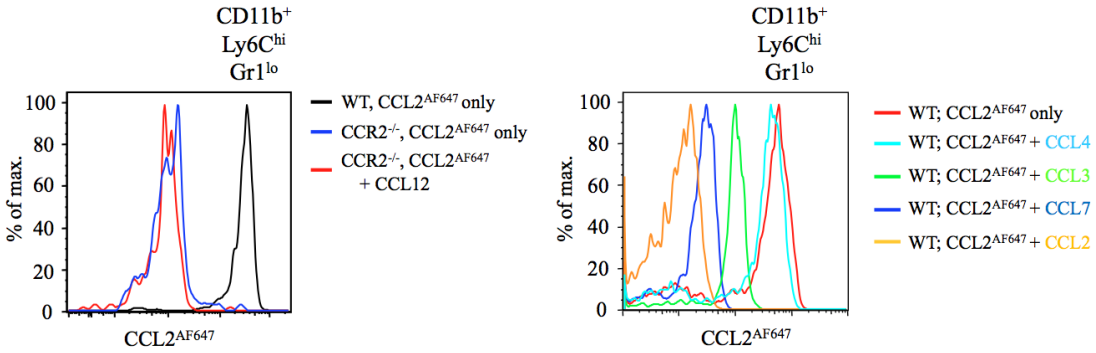

Supplementary Figure 6: CCL3 blocks CCR2-dependent CCL2^{AF647} uptake by splenic monocytes. WT or CCR2-deficient (CCR2$^{-/-}$) splenocytes were incubated at 37^{o}C with 10nM CCL2^{AF647} (+/-100nM of the unlabelled chemokines indicated), then at 4^{o}C with Abs against CD11b, Ly6C and Gr1. CCR2$^+$ splenic monocytes were identified as CD11b$^+$Ly6C^{hi}Gr1^{lo}. Cells were analysed by flow cytometry, with dead cell exclusion. The overlaid histogram plots show representative data from 5 repeat experiments.

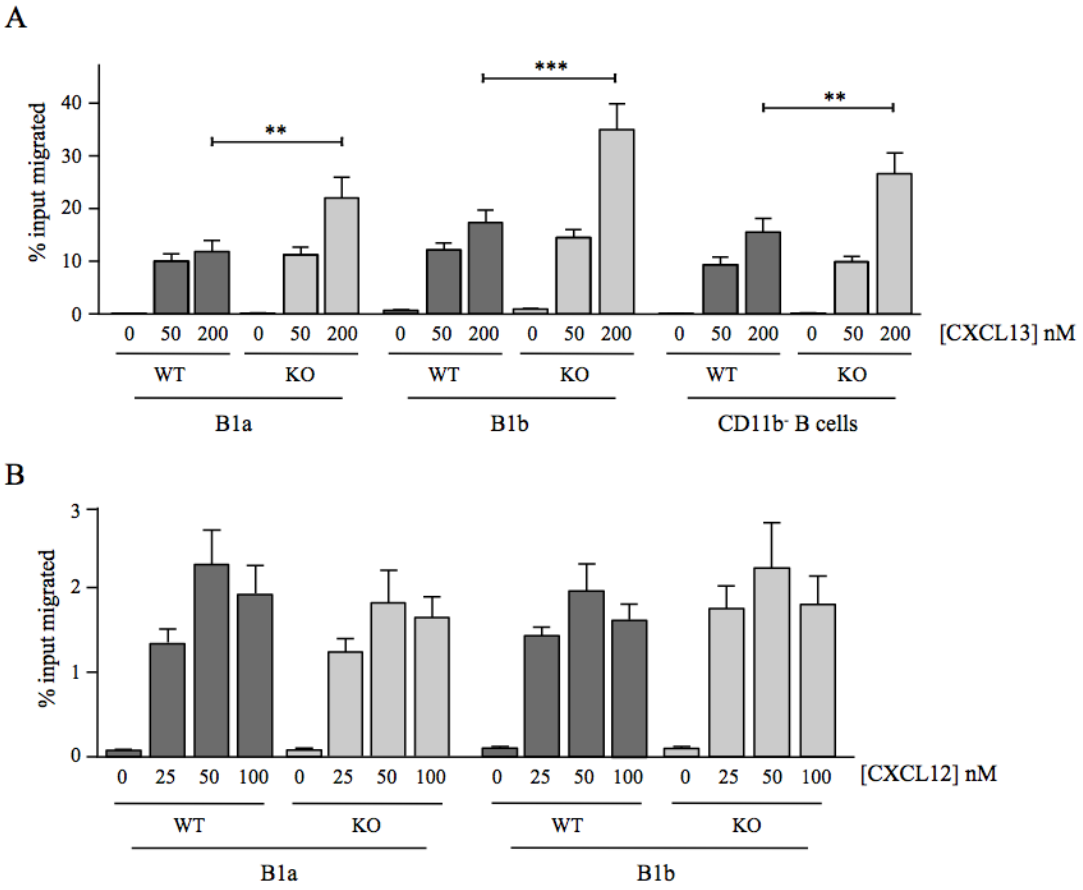

Supplementary Figure 7: Migration of WT and D6 deficient PerC B cells towards CXCL13 and CXCL12. Migration was assessed in Transwell chemotaxis chambers using $5x10^5$ input PerC cells (pooled from 3-4 WT or D6-deficient (KO) mice). Media alone (0), or the indicated concentrations of CXCL13 (A) or CXCL12 (B), were present in the lower chamber of the chemotaxis plate. The cells that migrated into the lower chamber were phenotyped (using antibodies against CD19, CD11b and CD5) and enumerated by flow cytometry. Data are presented as the mean number of live cells migrated (as percent of input) (+/-SEM) from three or more replicates. Repeat experiments generated similar datasets. ** $p<0.01$; *** $p<0.001$.

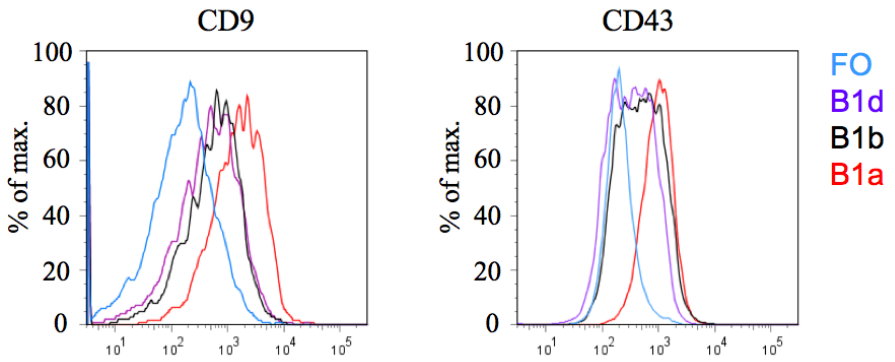

Supplementary Figure 8: Surface expression of CD9 and CD43 on various PerC B cell subsets. WT PerC cells were incubated at 4°C with Abs against CD19, CD11b, CD23 and CD5 (to identify specific B cell subsets), and either CD9 or CD43, and then analysed by flow cytometry. CD9 and CD43 profiles are shown for live cells within each of the B cell subsets indicated and are representative of data generated from at least three repeat experiments.

B cell Subset	Surface Immunophenotype (CD19, CD11b, CD5 & CD23)	Pleural Cavity (% of B cells)	Peritoneal Cavity (% of B cells)	**D6 activity**
B1a^{23+}	CD19+ CD11b+ CD5+ CD23+	1.28+/-0.16	0.72+/-0.22	+
B1a	CD19+ CD11b+ CD5+ CD23-	25.46+/-1.13	29.86+/-6.95	+
B1b^{23+}	CD19+ CD11b+ CD5- CD23+	12.76+/-1.70	4.74+/-0.53	+
B1b	CD19+ CD11b+ CD5- CD23-	23.41+/-2.48	20.29+/-6.29	+
B1c^{23+}	CD19+ CD11b- CD5+ CD23+	1.41+/-0.48	1.51+/-0.51	+
B1c	CD19+ CD11b- CD5+ CD23-	11.55+/-1.84	11.15+/-3.05	+
FO	CD19+ CD11b- CD5- CD23+	13.00+/-0.57	21.27+/-7.71	-
B1d^{23+}	CD19+ CD11b- CD5- CD23+	3.60+/-1.07	1.92+/-0.61	+
B1d	CD19+ CD11b- CD5- CD23-	5.34+/-0.37	6.51+/-0.91	+

Supplementary Table 1: The surface phenotype, relative abundance, and D6 activity of body cavity B cell subsets retrieved from WT C57Bl6 mice. Abundance data are presented as the mean percentage (+/-SD) of each subset within the CD19^{+} B cell population.